Georgia Journal of Science

Volume 81 *No. 2 Scholarly Contributions from the Membership and Others* Article 12

2023

Comparing a Georgia Reservoir With Solar-Powered Mixers to Another Without Mixers: Assessing Thermal and Oxygen Saturation and Nutrient Dispersion

Melissa Hage
Oxford College of Emory University, melissa.hage@emory.edu

Jordan Hasty
Oxford College of Emory University, jordan.elliott.hasty@emory.edu

Hannah Miller
Oxford College of Emory University, hannah.m.rose03@gmail.com

Comparing a Georgia Reservoir With Solar-Powered Mixers to Another Without Mixers: Assessing Thermal and Oxygen Saturation and Nutrient Dispersion

Acknowledgements

We would like to thank Oxford College of Emory University for financially supporting this research. We would also like to thank the following student researchers that helped advance this project – Camilla Kline, Julia Danko, Yaling Covey, Ayaka Smart, and Stella Rae Kinard. Essentially information about Lake Varner was provided by Bob Snipes, Assistant Water Production Manager with the Newton County Water System, and about Hard Labor Creek Reservoir by Jimmy Parker, PE, project manager for Hard Labor Creek Reservoir. This manuscript was substantially improved thanks to the help of Dr. Sarah Cadieux, Emily Kelly, and three anonymous reviewers.

COMPARING A GEORGIA RESERVOIR WITH SOLAR-POWERED MIXERS TO ANOTHER WITHOUT MIXERS: ASSESSING THERMAL AND OXYGEN STRATIFICATION AND NUTRIENT DISPERSION

Melissa M. Hage, Jordan Hasty, and Hannah Miller
Department of Environmental Sciences
Oxford College of Emory University
810 Whatcoat St., Oxford, Georgia, 30054
Corresponding author: Melissa.hage@emory.edu

Abstract

Harmful algal blooms (HABs) have been increasing over the last 50 years due to anthropogenic nutrient enrichment and increasing temperatures. One HAB control method is the use of solar-powered mixers. In this study we investigated the timing of thermal stratification, depth of the thermocline and oxycline, and dispersion of nutrients within the water column by comparing two reservoirs in Georgia, U.S.A. over a three-year period – Lake Varner (LV), which utilizes mixers, and Hard Labor Creek Reservoir (HLCR), which does not. Our data show that the onset of thermal stratification is within ± 2 days and appears at the same depth within both reservoirs. The timing of fall turnover consistently occurred one month earlier in LV than in HLCR. Both reservoirs had similar oxygen profiles during stratification, but in LV, dissolved oxygen levels increased more quickly in autumn compared to HLCR in all years. Both reservoirs had similar nutrient concentrations throughout the years and water column. These findings suggest the thermal, oxygen, and nutrient dynamics in the reservoirs are similar, despite LV having solar-powered mixers. Any differences can be attributed to LV being a slightly smaller and shallower reservoir.

***Keywords**:* Thermocline, oxycline, dissolved oxygen, total phosphorous, nitrate

INTRODUCTION

Cyanobacterial harmful algal blooms (HABs) have been increasing in frequency for at least 40-50 years and are expected to continue to increase due to ongoing anthropogenic nutrient enrichment and increasing global temperatures (Heisler et al. 2008; Paerl et al. 2011; O'Neil et al. 2012; Upadhyay et al. 2013; Huisman et al. 2018; Ho and Michalak 2020; Paerl et al. 2020; Smucker et al. 2021). When a reservoir becomes enriched in nutrients, most commonly nitrogen and phosphorous, eutrophication can occur and lead to an increasing amount of algal growth (Hecky and Kilham 1988; Schindler et al. 2008; Maberly et al. 2020). In reservoirs, P and N can be loaded both internally through organisms' interaction with their environment (Cottingham et al. 2015) and sediment release (Mortimer 1941; Mortimer 1942; Boström et al. 1988; Hupfer and Lewandowski 2008; Tammeorg et al. 2020), and externally from point sources, such as municipal sewage waste facilities, and nonpoint sources, such as agricultural runoff (Hudnell 2010). Warm water temperatures favor cyanobacteria growth over other species of phytoplankton, increasing likelihood of HABs (Wagner and Adrian 2009; Reinl et al. 2021). HABs can impact lake ecosystem function by limiting light penetration, decreasing oxygen levels, and producing toxins (Khan and Ansari 2005; Conley et al. 2009; Chislock et al. 2013). These processes can have severe ecological, economic, and societal impacts, as they are detrimental to important ecosystem services including wildlife habitat, carbon sequestration, hydrological buffering and regulation, sediment and nutrient retention and processes, water usage for irrigation and drinking water, and recreational use (Schallenberg et al. 2013; Zhong et al. 2019; Sterner et al. 2020).

Convective mixing and the structure of thermal stratification, alongside wind-induced currents, are the main controllers of the vertical distribution of heat, dissolved substances, and nutrients in the water column of lakes (Elçi 2008; Yang et al. 2018; Mesman et al. 2021). In lake areas deeper than about 3 – 3.5 m, warm air temperature and sunlight can lead to a temperature gradient in the water column that creates a physical force strong enough to resist the wind's mixing forces. The lake stratifies into cooler bottom waters (hypolimnion), warmer upper waters (epilimnion), and a transitional metalimnion where there is a steep thermal gradient. Increasing global temperatures continue to warm surface temperatures of lakes, which intensifies and lengthens the period of thermal stratification (Adrian et al. 2009; Williamson et al. 2009; O'Reilly et al. 2015; Niedrist et al. 2018; Reinl et al. 2021). Stratification during the summer acts as a barrier restricting mixing of the water column. The warm water in the epilimnion is unable to move into the cold, dense water of the hypolimnion. As a result of incomplete mixing of the water column and lack of light for photosynthesis in the hypolimnion, this portion of the water column can become anoxic. Stratification is weakened by natural convection when surface water cools. The vertical descent of this denser, cooled water leads to the nightly formation of a mixed surface layer and the seasonal deepening of the surface layer that may culminate in full lake turnover.

The creation of an anoxic hypolimnion during stratification also influences nutrient concentrations, which can result in elevated HAB frequencies and intensities (Paerl et al. 2011; O'Neil et al. 2012; Paerl et al. 2020). In lakes that experience periods of hypolimnetic anoxia, internal phosphorous loading takes on an important role. At low oxygen concentrations, the sediment Fe(III) is reduced to Fe(II). This results in the breakdown of Fe-P complexes and the dissolution of the associated phosphate into overlying lake water. Fall lake turnover provides a mechanism for transferring these nutrients up into the photic zone where they may support cyanobacterial productivity (Mortimer 1941; Mortimer 1942; Boström et al. 1988; Hupfer and Lewandowski 2008; Tammeorg et al. 2020).

Artificial mixing has been used for many years to reduce the presence and impact of HABs. Artificial mixers facilitate a change from cyanobacterial dominance to green algae and diatoms by decreasing the stability of the water column. Many species of cyanobacteria have positive buoyancy mechanisms that allow them to remain shallower in the water column to receive more light than other negatively buoyant phytoplankton. Negatively buoyant phytoplankton, including many green algae and diatoms, have population losses due to sinking and sedimentation losses. Artificial mixing prevents sedimentation losses of desirable phytoplankton, while creating more turbulent mixing conditions that lead to a lower light dose for buoyant cyanobacteria. The net effect is a decrease in the population of cyanobacteria as compared to green algae and diatoms (Reynolds 2006; Visser et al. 2016; Huisman et al. 2018; Reinl et al. 2021). Solar-powered mixers differ from other artificial mixing regimes in that the goal is to reduce HABs by only mixing the epilimnion, instead of fully mixing the water column and dissolving lake stratification.

Solar-powered mixers are often appealing to lake managers for their potential to reduce HABs, which is why much of the published literature focuses on the beneficial effects of artificial mixing on controlling HABs. However, there is a lack of investigations on the potentially larger implications of the use of these mixers on overall lake temperature, oxygen, and nutrient dynamics. Therefore, the goal of this project is not to determine the impact of solar-powered mixers on HABs or other biological components, but rather the mixers impact on the timing of thermal stratification, the depth of the thermocline and oxycline, and the dispersion of nutrients within the water column. This is accomplished by comparing two similar reservoirs, of which only one has solar-powered mixers. Although the scope of the investigation is spatially limited (i.e., data comes from a single location in each lake), we have compiled a comprehensive dataset spanning three full years. While preliminary, our conclusions can begin to address the current knowledge gap regarding the effects of solar-powered mixers on the physical and chemical dynamics of reservoirs. It is critical to gain a thorough understanding of these dynamics throughout the entire water column for assessing both the overall health of the ecosystem and ensuring the implementation of solar-powered mixers do not have a negative impact on natural temperature, nutrient, and oxygen levels dynamics, which are essential for reservoir health.

MATERIALS AND METHODS

Site Description

The state of Georgia, USA, has very few naturally occurring lakes; instead, reservoirs make up over 99% of its freshwater lentic systems (Cowie et al. 2002; Parker 2019). Both Hard Labor Creek Reservoir (HLCR) and Lake Varner (LV) are classified as warm monomictic reservoirs and are located in the Georgia Piedmont province (Figure 1). The Piedmont is Georgia's most populous region, with more than 4.5 million inhabitants (Atlanta Regional Commission 2022). The region is characterized by rolling hills, shallow valleys, and red clay soil. Additionally, it is underlain by late Paleozoic igneous and metamorphic rock. LV sits at an elevation of 215 m and HLCR is at 225 m. On average, the study area receives 1270 mm of precipitation annually (Rose and Peters 2001).

LV and HLCR were selected for study for their physical and geographic similarities, as well as logistical access. Both reservoirs have large, open water areas deep enough to allow thermal stratification, as well as being similar with respect to reservoir surface area, watershed size, and land-use within their watersheds. Land use was considered due to its potential impact on nutrient loading. Logistically, the managing bodies of both reservoirs granted us permission for long-term data collection. Additionally, both reservoirs are located within 30 km of the researchers' academic institution. Currently, time and resource limitations have resulted in the collection of data from only one location at each reservoir (Figure 1). However, we are in the process of establishing more temperature arrays and collection locations to better capture whole lake dynamics. No site-specific weather data are available for either location, however rainfall data were retrieved from the US National Weather Service.

Watersheds for both reservoirs were delineated using data from the United States Geologic Survey (USGS) National Hydrography Dataset, as well as digital elevation model data from the USGS 3D Elevation Program (U.S. Geological Survey 2013; U.S. Geological Survey 2019a; U.S. Geological Survey 2019b). The National Hydrography Dataset had watershed and waterbody shapes delineated for LV from 2013, but neither of these were

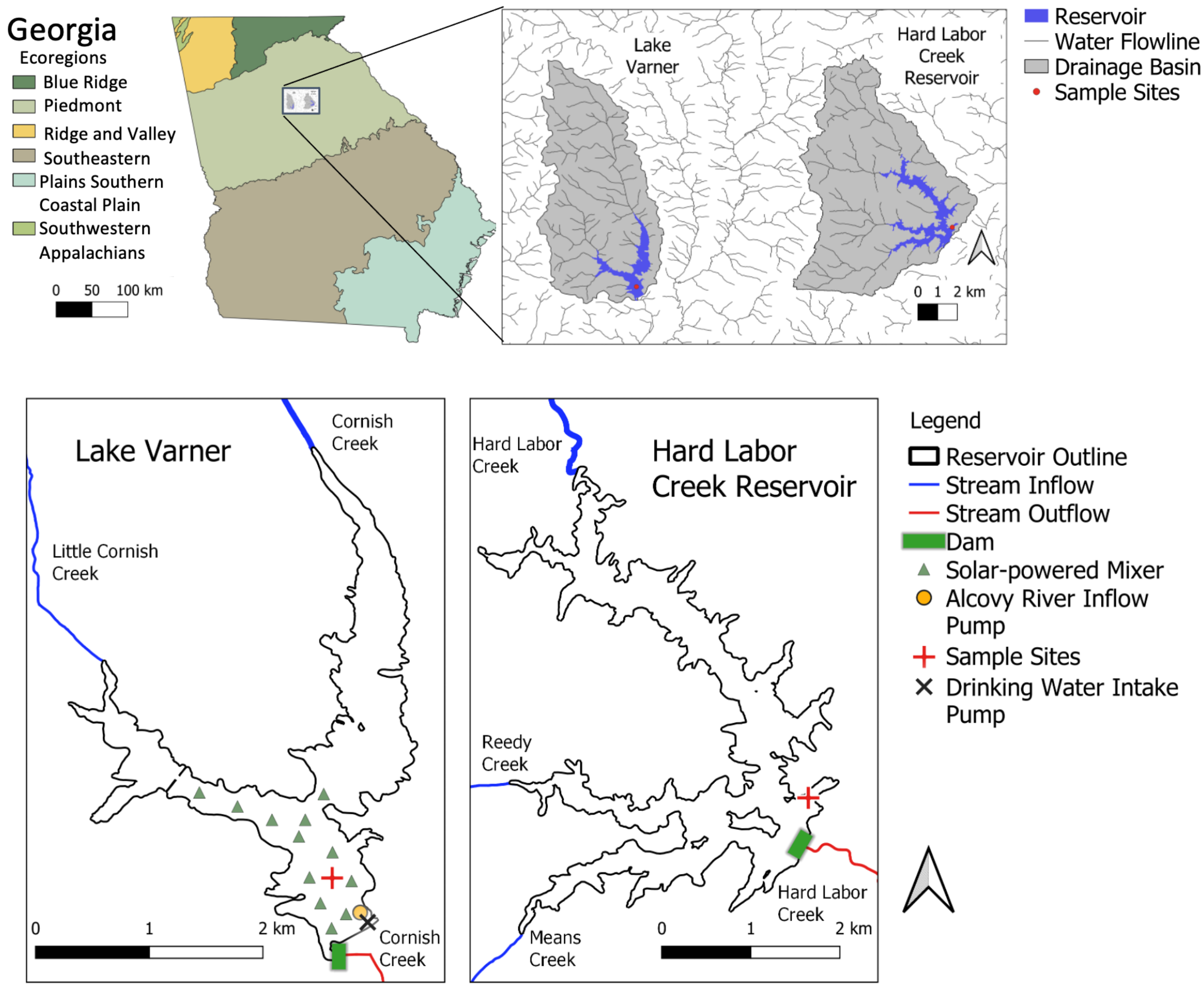

Figure 1. Location of the two reservoirs within the Piedmont of Georgia, the outline of each reservoir's watershed, and detailed site information about each reservoir.

delineated for HLCR. The digital elevation model was used to estimate how water would drain over the terrain. Using the estimated flowlines, the watershed for HLCR was manually digitized, and LV's watershed shape was visually verified. HLCR's waterbody was manually digitized using 2019 satellite imagery from the National Agricultural Imagery Program (USDA-FSA-APFO 2019a, USDA-FSA-APFO 2019b). Land-use characteristics were compared between watersheds using the 2019 Cropland Data Layer (CDL) from the United States Department of Agriculture (USDA) Cropscape data program (USDA National Agricultural Statists Service 2019). The CDL did not fully reflect the HLCR waterbody, so the waterbody shape as delineated from satellite imagery was overlaid onto the CDL.

Lake Varner (LV)

LV is an ~350 ha reservoir in Newton County, Georgia that opened in 1993 after the damming of Cornish Creek. It has an average depth of 5.5 m and a maximum depth of ~

11 m. The watershed of LV is 63.5 km^2 and is predominantly forested (58.8%) and grass/pastureland (24.4%), with only 7.1% developed area (Figure 2). In addition to rainfall and runoff into the Cornish Creek watershed, water is pumped from the nearby Alcovy River during periods of drought to meet water demand and stored in the reservoir (Figure 1). The total treatment capacity of LV is ~9.46×10^4 m^3 per day and allows Newton County to reliably access drinking water (About the Facility | Newton County, GA 2022).

In 2013, 12 SolarBee® lake circulators were deployed in LV for the purpose of strengthening mixing and reducing algal growth. Previously, cyanobacterial growth was managed using chemical control methods. These mixers are anchored in place to the bottom of the lake and are distributed throughout the main body of the reservoir (Figure 1). They have batteries so that they are able to run continuously throughout the day and night. SolarBee® mixers use an up-flow water circulator to pump water through an intake pipe with a diameter of 1.8 m at the bottom of the mixer from a depth of 3 m below the surface and distribute the water across the surface radially in a long-distance flow pattern. These mixers operate at the same flow rate of 39 m^3 per minute year-round.

No robust water column temperature, dissolved oxygen, or nutrient data is available prior to solar-powered mixer deployment to compare the direct impacts. Additionally, there have been no periods when the mixers were not operating, so no data are available to inform the "natural" mixing conditions within LV.

Hard Labor Creek Reservoir (HLCR)

The construction of the HLCR dam began in 2012 on the southeast side of Walton County, and the reservoir was filled by 2018. HLCR has a surface area of ~555 ha and a storage volume of ~4.54×10^7 m^3, indicating an average depth of 8 m. It has a max depth of 28 m near the reservoir's dam (Hard Labor Creek Regional Reservoir). The reservoir has a dendritic morphology, with multiple branches of varying depth. The cove in which our data were collected has a maximum depth of ~12 m. The watershed of HLCR is 77.3 km^2 and the land use is predominantly forested (51.8%) and grass/pastureland (28.6%), with only 9.5% developed areas (Figure 2). While no water is currently withdrawn from the reservoir, there are plans to construct the first water treatment facility onsite around 2023 – 2024 and deploy solar-powered mixers (J. Parker, personal communication, June 4, 2021). Data presented in this study from when mixers were not present in HLCR will allow for a better comparison of direct impacts of solar-powered mixers on lakes after the mixers have been installed.

Data Collection and Analysis

From January 2020 – December 2022, Onset Hobo Pendant® MX Water Temperature Data Loggers were deployed at one-meter increments along a 10-meter-deep array in each reservoir. The measurement accuracy of these sensors is ±0.5°C from -20° to 70°C, with 0.04°C resolution. The sensor array in LV was located at least 60 m from any of the installed solar-powered mixers. Each sensor collected a temperature value every two hours. Temperature arrays were checked monthly, and all data were offloaded at that time. Once logged, daily averages were calculated from the two-hour readings at each depth for each reservoir and were used to create annual heatmaps. For the purposes of this study, a thermocline is present when the difference between seven-day average temperatures at adjacent depths exceeds 1°C (Wetzel 2001) and persists for at least 10

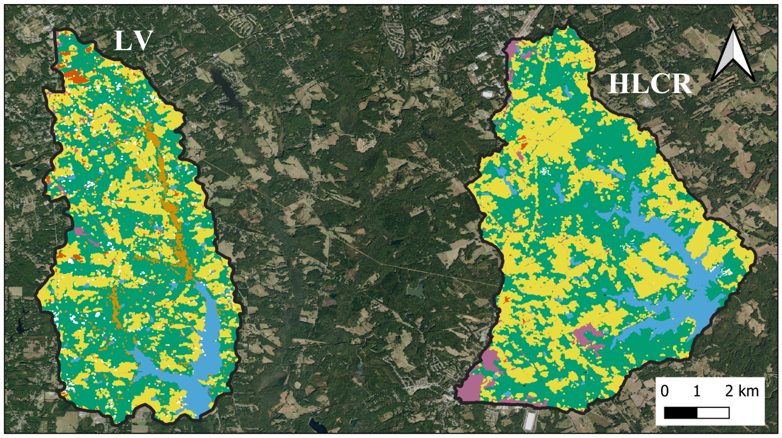

Land Use	% of watershed covered	
	LV	HLCR
Forest	58.8	51.8
Grass/Pasture	24.4	28.6
Developed	7.1	9.5
Open water	6.1	7.7
Wetlands	2.0	1.0
Row crop	0.7	0.7
Other	0.9	0.7

Figure 2. Watershed delineation and land-use determination for Lake Varner and Hard Labor Creek Reservoir.

days. Mean temperatures from each reservoir from depths of 1, 3, 6, and 9 m were compared when the reservoirs were stratified (April – September), in fall transition (October – November), and mixed (December – February).

The data loggers were occasionally prone to failure. These failures were identified, and sensors replaced at the monthly collections, a total of 110 times (averaging 1.5 per reservoir per month), which resulted in missing 17% of daily average temperature over three years. To mitigate this, in cases where temperatures were available at depths adjacent to missing data, nearby datapoints were used to interpolate the missing values. For example, if the values immediately above and below were both present, an average of the two was calculated. If data were missing at two or three consecutive depths, a linear interpolation was done between the nearest available temperatures. Collectively, this technique filled in all but 2% of the missing data, which were instances of data missing from one of the ends of the sensor array (i.e., 1 m or 10 m depth). While interpolation was used, extrapolation was not. To validate the interpolation, the same calculations were applied to non-missing measurements and compared to the actual values. Based on this validation, 90% of all heatmap data, including actual measurements and interpolated values, was estimated to be within 0.5 °C of the actual temperature.

When temperature data were retrieved each month, an In-Situ smarTROLL Multiparameter Handheld Sonde was also utilized to collect dissolved oxygen (DO) concentrations. The measurement accuracy of this instrument is ±0.2 mg/L from 0 to 8 mg/L, with 0.01 mg/L resolution. From January 2020 – May 2020, data were collected only from depths of 1, 3, 6, and 9 m in each reservoir at the same location as the temperature array. Starting in June 2020, data were collected at one-meter increments along the entire length of the ten-meter array at each reservoir. For all data collection, readings were recorded at each depth every ten seconds for ~ 60 seconds and an average value for each parameter was calculated. For the purposes of this study, the oxycline is defined as the greatest decrease of DO concentrations between 1 m intervals, so long as that difference exceeds 1 mg/L/m.

Water samples for *ex situ* analysis were collected once each month from 1, 3, 6, and 9 m depths from each reservoir using a horizonal Van Dorn water sampler. Concentrations of nitrate-nitrogen (NO_3^- –N) and total phosphorous (PO_4^{-3}-P) were determined by analyzing a single water sample from each collection event using a HACH

DR3900 spectrophotometer. Photometric measuring range is ±3.0 Ab (wavelength range 340 – 900 nm) and photometric accuracy is 5 mAbs at 0.0 – 0.5 Abs and 1% at 0.50 – 2.0 Abs. A cadmium reduction method was used to determine NO_3^- –N concentrations, with a detection limit of 0.1 mg/L (Hach Company 2014). PO_4^{-3}-P concentrations were determined using the low-range USEPA PhosVer® 3 with Acid Persulfate Digestion Method (EPA 365.3; USEPA, 1978), which has a detection limit of 0.06 mg/L.

RESULTS

Temperature

Lake Varner (LV)

The maximum reservoir temperatures in LV for 2020 – 2022 were 32.2°C, 31.9°C, and 31.7°C, respectively. These temperatures were all recorded at a depth of 1 m between the last week of June and the end of July. The minimum reservoir temperatures in LV for 2020 – 2022 were 8.0°C, 7.4°C, and 6.8°C, respectively. These temperatures were recorded at depths between 6 and 9 m between the end of December and early February. Thermal stratification in LV was established on March 12, 2020 (2 – 3 m), March 13, 2021 (3 – 4 m), March 30, 2022 (7 – 8 m). In mid-April to mid-May 2020, the thermocline disappeared before reappearing and staying present until fall turnover. The location of the thermocline deepened throughout the summer and fall, before disappearing on November 1, 2020, October 28, 2021, and October 20, 2022 (Figures 3A, 4A, and 5A).

Hard Labor Creek Reservoir (HLCR)

Between 2020 – 2022, the maximum reservoir temperatures in HLCR were 32.5°C, 32.1°C, and 32.4°C, respectively. These temperatures were recorded at a depth of either 1 or 2 m, between the middle of June through the start of August. The minimum reservoir temperatures in HLCR were 9.4°C, 8.1°C, and 8.0°C, respectively, and were recorded at a depth of 7 or 8 m between the end of December and early February. HLCR became thermally stratified on March 11, 2020 (2 – 3 m), March 11, 2021 (3 – 4 m), and March 21, 2022 (7 – 8 m) and stayed stratified until November 28, 2020, November 23, 2021, and November 18, 2022, with the thermocline getting progressively deeper until it disappeared (Figures 3B, 4B, and 5B).

Comparison

During periods of stratification (April – September) and during the fall transition (October – November), mean water temperatures at depths of 1 m and 3 m in all three years were warmer in HLCR than in LV (Table 1). However, the mean difference in daily readings from corresponding depths was never greater than 0.4°C during these periods. During periods of stratification, the mean difference in daily temperature in HLCR was 1.2°C colder at 6 m and 3.7°C colder at 9 m than in LV. During fall turnover, the mean difference in daily temperature in HLCR was 3.0°C colder at 9 m than in LV. When the reservoirs were mixed (December – February), mean water temperatures at depths of 1 m, 3 m, 6 m, and 9 m across all three years were warmer in HLCR than in LV. However, the mean difference in daily readings from corresponding depths was never greater than 0.5°C.

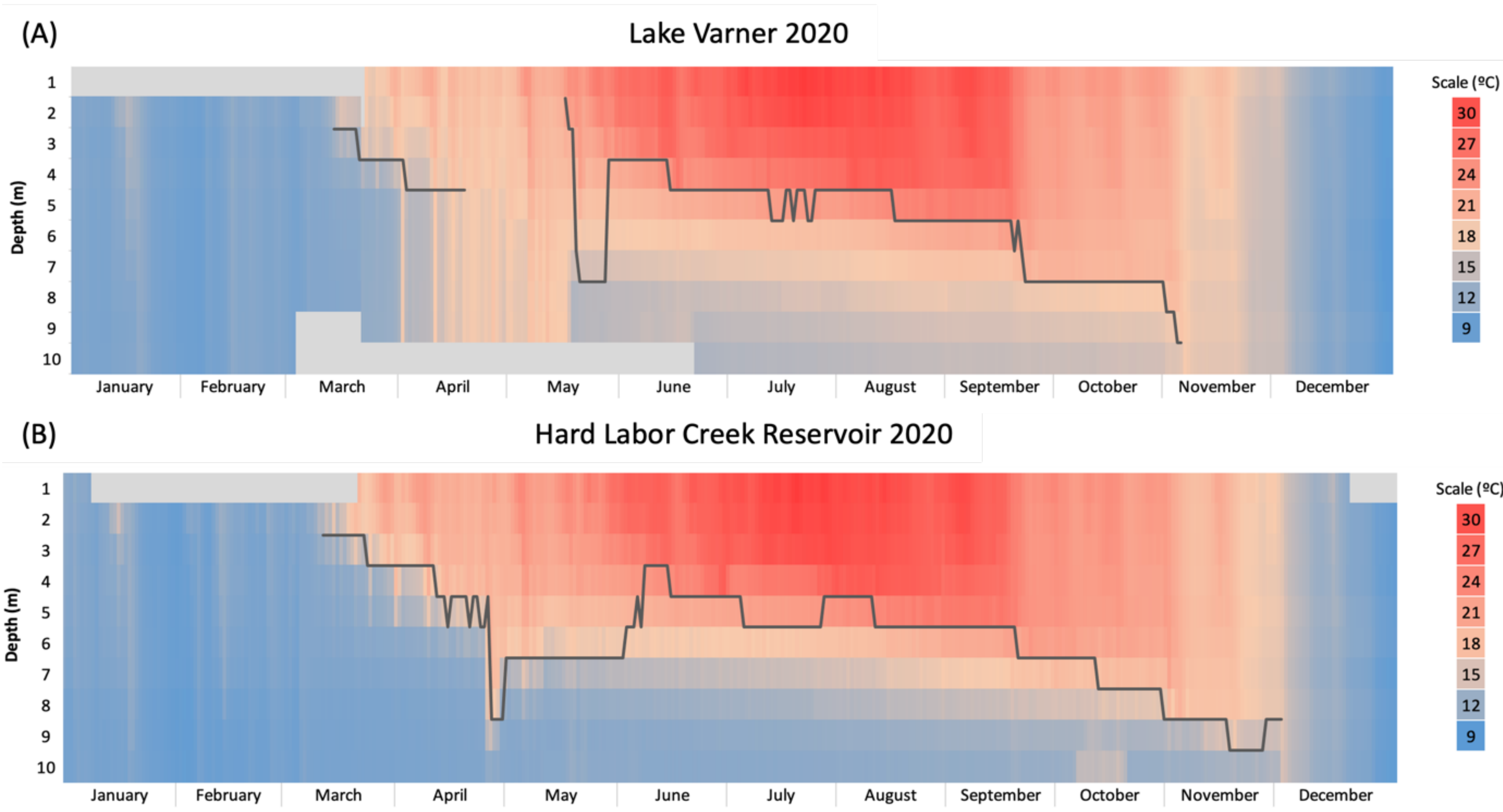

Figure 3. Heat maps of daily average temperatures for Lake Varner (A) and Hard Labor Creek Reservoir (B) for 2020. The solid line represents the thermocline. A break in the solid line represents a time period when the thermocline temporarily disappeared.

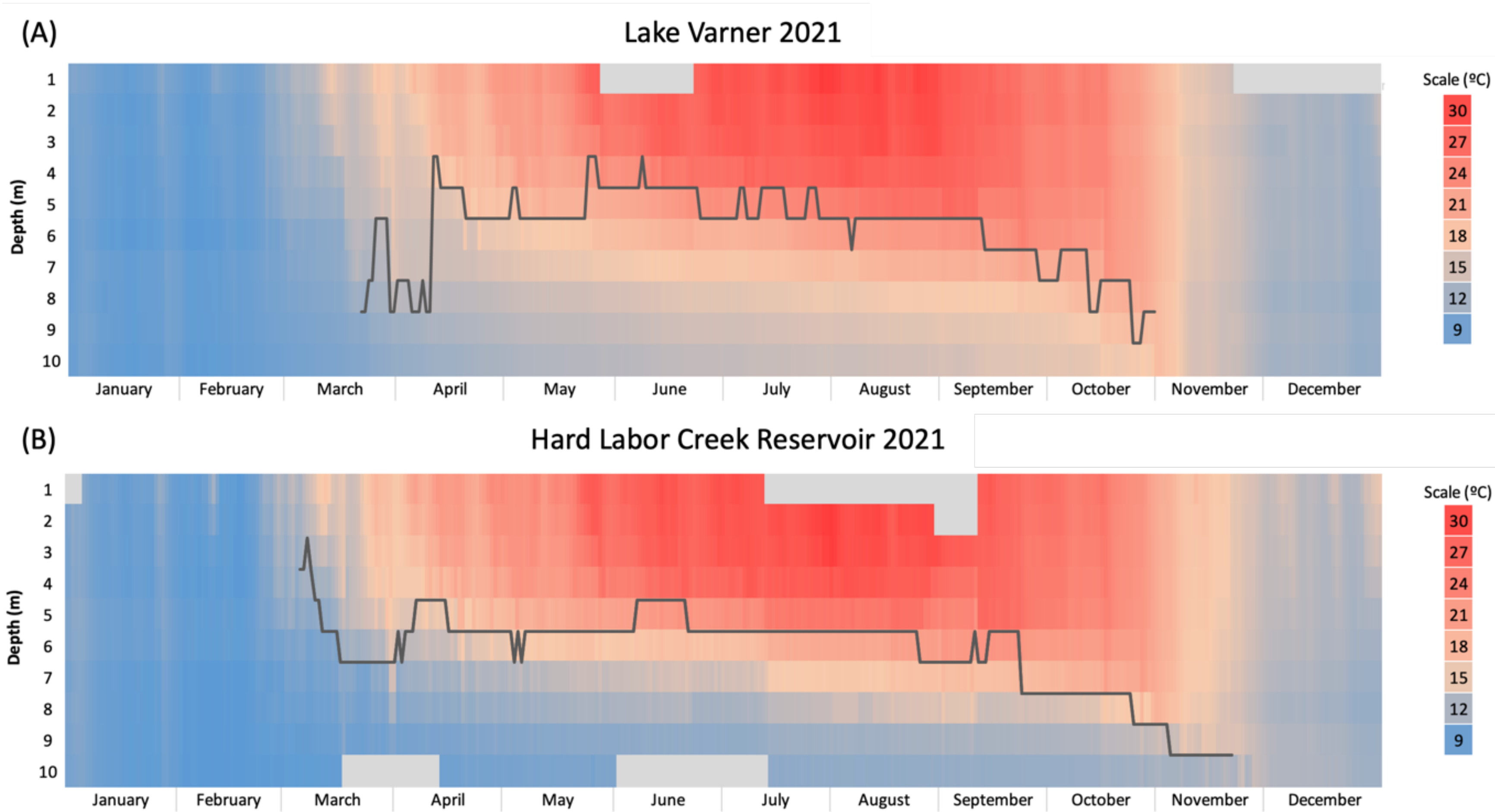

Figure 4. Heat maps of daily average temperatures for Lake Varner (A) and Hard Labor Creek Reservoir (B) for 2021. The solid line represents the thermocline.

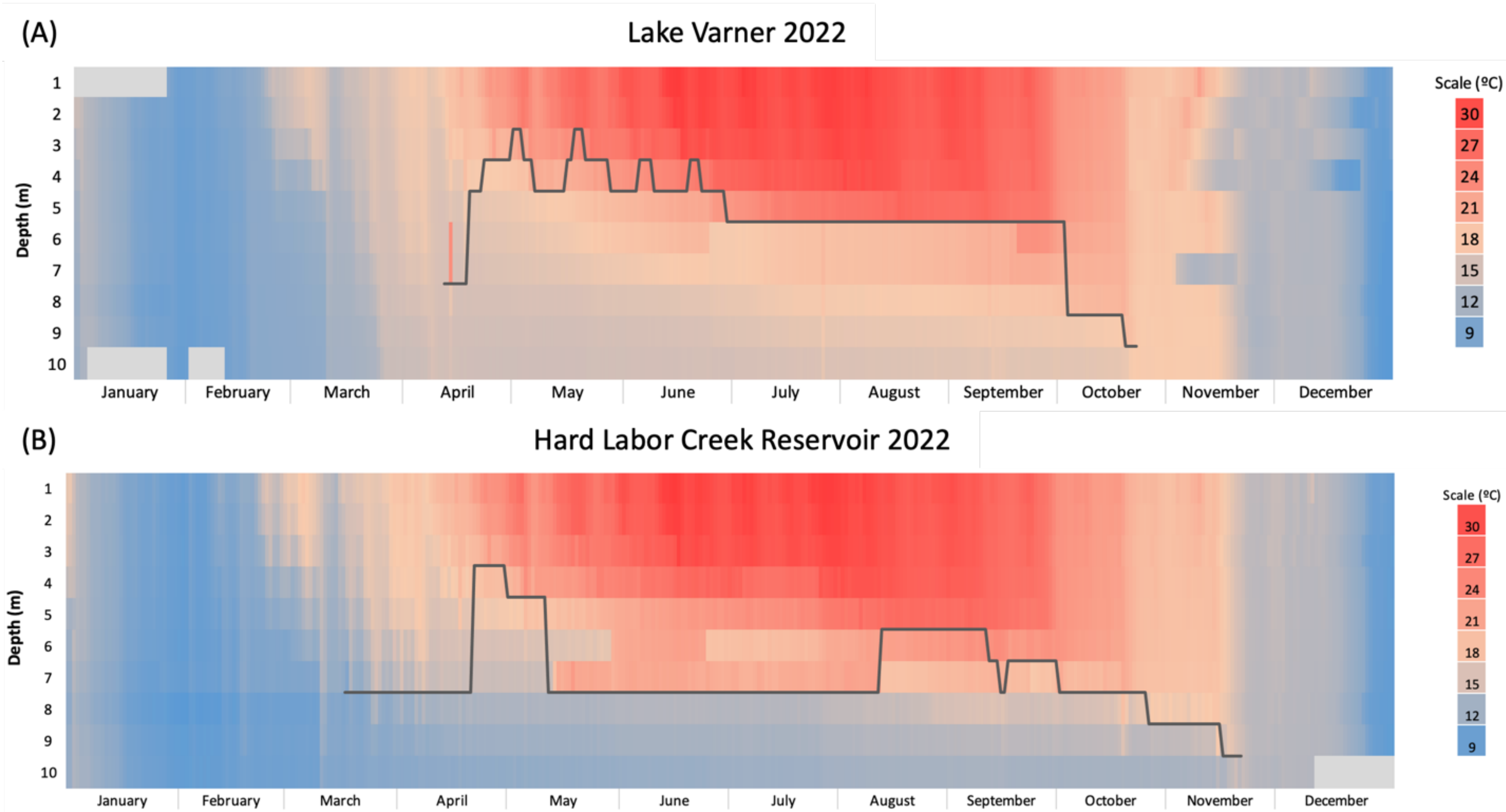

Figure 5. Heat maps of daily average temperatures for Lake Varner (A) and Hard Labor Creek Reservoir (B) for 2022. The solid line represents the thermocline.

Table 1. Mean temperatures during the 3-year study period (2020 – 2022) at different depths during periods of stratification, fall turnover, and when the reservoirs are mixed.

		1 m (°C)	3 m (°C)	6 m (°C)	9 m (°C)
Stratified (Apr.–Sep.)	Lake Varner	26.16 ± 4.30	25.40 ± 4.16	19.07 ± 2.24	15.40 ± 1.24
	Hard Labor Creek Res	26.29 ± 4.24	25.73 ± 4.25	17.87 ± 2.84	11.69 ± 0.90
Turnover (Oct.–Nov.)	Lake Varner	19.71 ± 3.25	18.81 ± 3.44	18.43 ± 2.91	16.60 ± 1.60
	Hard Labor Creek Res	19.79 ± 3.22	19.15 ± 3.27	18.39 ± 2.61	13.62 ± 0.82
Mixed (Dec.–Feb.)	Lake Varner	10.33 ± 2.01	10.37 ± 1.71	10.10 ± 1.73	10.12 ± 1.62
	Hard Labor Creek Res	10.75 ± 1.92	10.84 ± 1.63	10.61 ± 1.46	10.28 ± 1.53

Dissolved Oxygen (DO)

Lake Varner (LV)

Between 2020 – 2022, DO concentrations ranged from 0 to 10.1 mg/L, 10.4 mg/L and 10.6 mg/L, respectively. Peak oxygen concentrations were observed in March 2020 at 1 m, February 2021 at 3 m and 4 m, and February 2022 at 2 m. The entire water column was oxygenated (greater than 1 mg/L) during the annual period of reservoir mixing (November – April) in all three years. An oxycline was established by March and persisted through November, displaying a clinograde oxygen curve (Figures 6A, 7A, and 8A).

Hard Labor Creek Reservoir (HLCR)

Between 2020 – 2022, DO concentrations ranged from 0 to 9.7 mg/L, 10.2 mg/L, and 9.6 mg/L, respectively. Peak oxygen concentrations occurred in March in all three years, at a depth of 1 m in 2020 and 2021 and a depth of 2 m in 2022. The entire water column was oxygenated (greater than 1 mg/L) during the annual period of reservoir mixing (November – April) in all three years. An oxycline was present from March to November, displaying a clinograde oxygen curve during all three years (Figures 6B, 7B, and 8B).

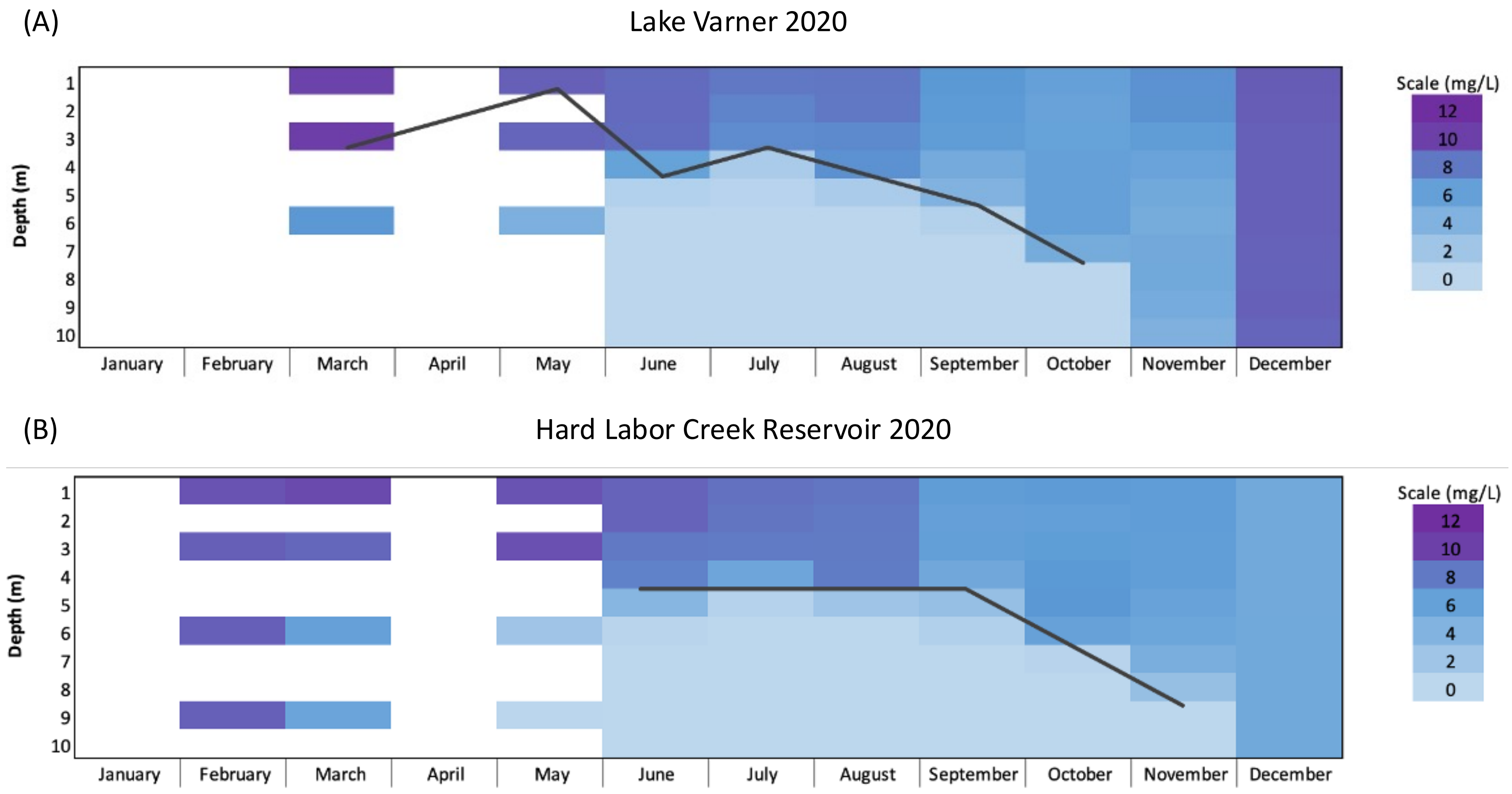

Figure 6. Dissolved oxygen (DO) concentrations sampled monthly throughout the 10 m water column of Lake Varner (A) and Hard Labor Creek Reservoir (B) in 2020. The DO measurements were recorded at 3 m depth intervals during the first 5 months of the year (January – May) and recorded at 1 m depth intervals for the remainder of 2020 (June – December). No data were collected in January and April 2020. The solid line represents the oxycline.

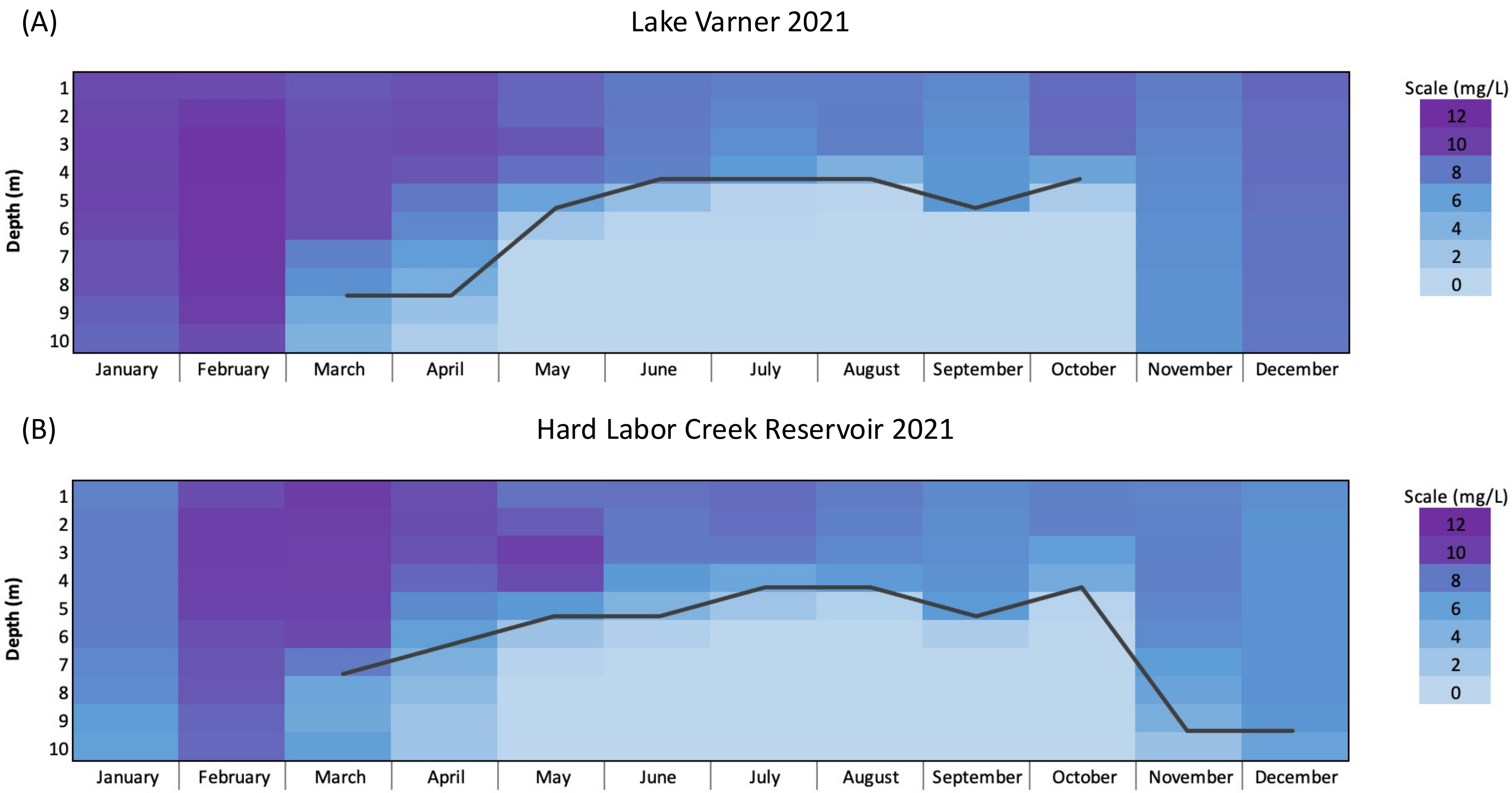

Figure 7. Dissolved oxygen (DO) concentrations sampled monthly throughout the 10 m water column of Lake Varner (A) and Hard Labor Creek Reservoir (B) in 2021. The DO measurements were recorded at 1 m depth intervals. The solid line represents the oxycline.

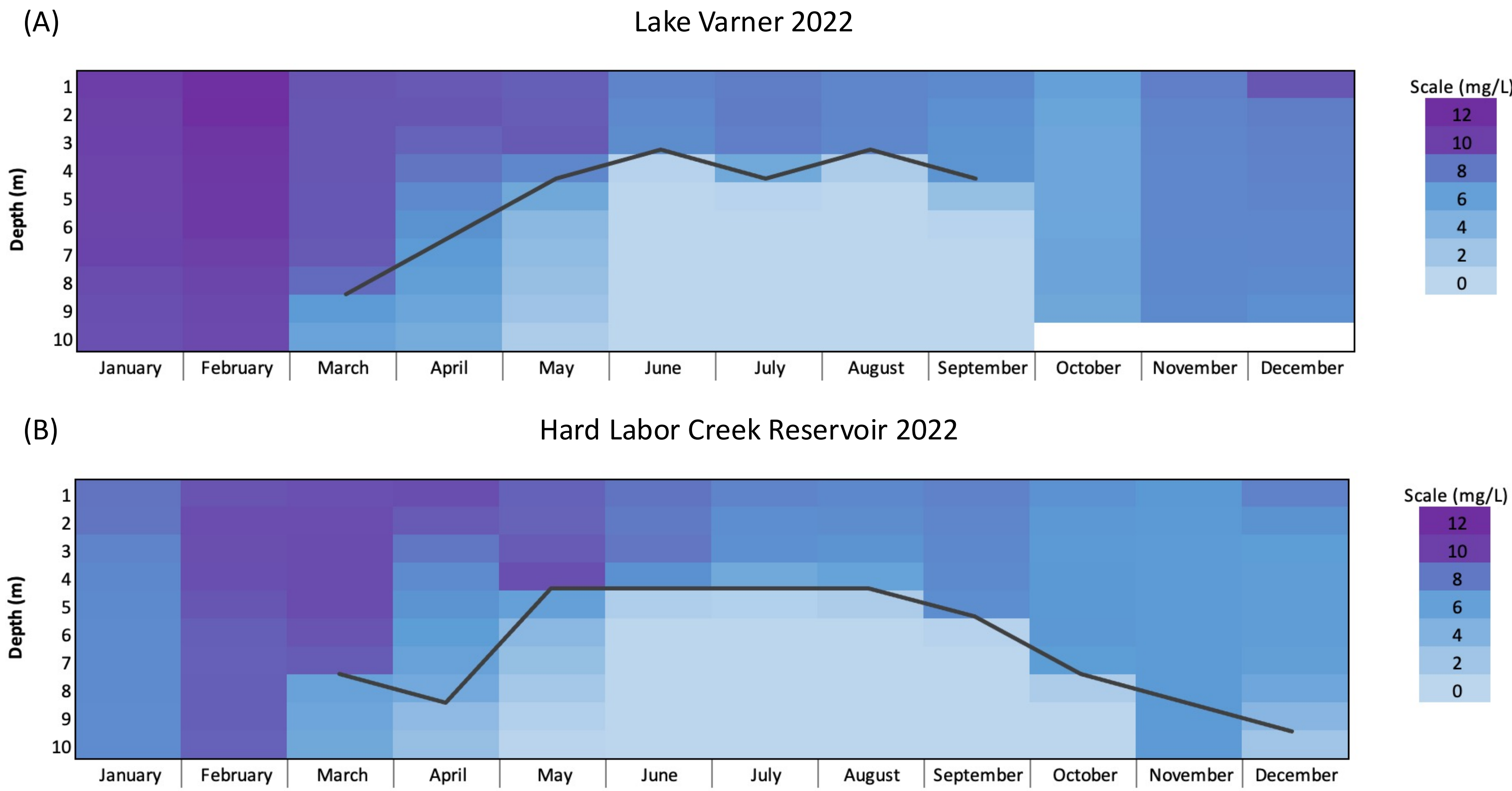

Figure 8. Dissolved oxygen (DO) concentrations sampled monthly throughout the 10 m water column of Lake Varner (A) and Hard Labor Creek Reservoir (B) in 2022. The DO measurements were recorded at 1 m depth intervals. The solid line represents the oxycline.

Oxygen Saturation

During thermal stratification in both reservoirs, DO levels in the epilimnion were consistently within 1 mg/L of saturation values (Figure 9A). In many cases, DO values exceeded the saturation point, reaching oxygen supersaturation levels up to 125%. In the metalimnion and hypolimnion, DO concentrations begin decreasing as thermal stratification was initiated, starting from around 2.5 mg/L below saturation levels in February of all three years and reaching values near 0 mg/L by May (Figure 9B and 9C).

In the epilimnion, maximum DO levels (between 9.5 and 10.6 mg/L) were observed around the time of initial stratification each year. From there they steadily decreased by an average of 0.40 mg/L/month in LV and 0.46 mg/L/month in HLCR each summer, reaching minimum values (between 5.2 and 7.4 mg/L) during the autumn turnover. When the reservoirs became fully mixed by December, DO concentrations in both reservoirs' epilimnions began increasing again by an average of 0.91 mg/L/month in LV and 1.11 mg/L/month in HLCR, reaching saturation by March as the reservoirs began to warm (Figure 9A).

During the fall turnover periods, DO levels in the metalimnion and hypolimnion increased, but did not reach or exceed saturation values. In both reservoirs in all three years, hypolimnetic DO rose from near 0 mg/L to within 1 mg/L of epilimnetic DO by December. However, this rate of increase in oxygen concentrations in the metalimnion and hypolimnion was greater in LV than in HLCR for all three years (Figures 9B and 9C). For example, in 2020 at HLCR, the oxygen concentration in the hypolimnion increased by 5.2 mg/L over 2 months, going from 0.1 mg/L in October to 5.3 mg/L in December (Figure 9C). The oxygen concentration in the hypolimnion in LV increased by 8.8 mg/L over the same time, going from 0.1 mg/L in October to 8.9 mg/L in December. In HLCR, DO levels of this magnitude were not reached until February 2021. In February 2021, LV's oxygen concentration had further increased to its maximum at 10.1 mg/L. In both lakes, hypolimnetic DO continued to increase after full mixing in December, tracking or lagging slightly behind epilimnetic DO, before beginning to decrease again with spring stratification. (Figure 9B and 9C).

Nutrients

Lake Varner (LV)

Maximum NO_3^- –N concentrations were 1.4 mg/L (2020) and 0.4 mg/L (2021 and 2022), with 90% of values across all years being below 0.5 mg/L (Figure 10A). Concentrations were generally stable throughout the water column, however, there were a few instances in 2020 when concentrations decreased with depth. Generally, the lowest NO_3^-–N values were measured during the summer months. The highest NO_3^- –N concentrations found throughout the entire water column were measured on December 17, 2020, when values ranged from 0.5 – 1.4 mg/L (Figure 10A).

Maximum PO_4^{-3}–P concentrations were 0.6 mg/L (2020), 1.1 mg/L (2021), and 1.3 mg/L (2022) with 90% of values across all years being below 0.7 mg/L. Overall, PO_4^{-3}–P concentrations were not depth dependent, with values relatively stable throughout the water column. Overall, the lowest PO_4^{-3}–P values were measured during the summer months. The highest concentrations were found throughout the water column in November 2022, with December 2020, January 2021, and August 2021, also being times of higher PO_4^{-3}–P concentrations (Figure 10C).

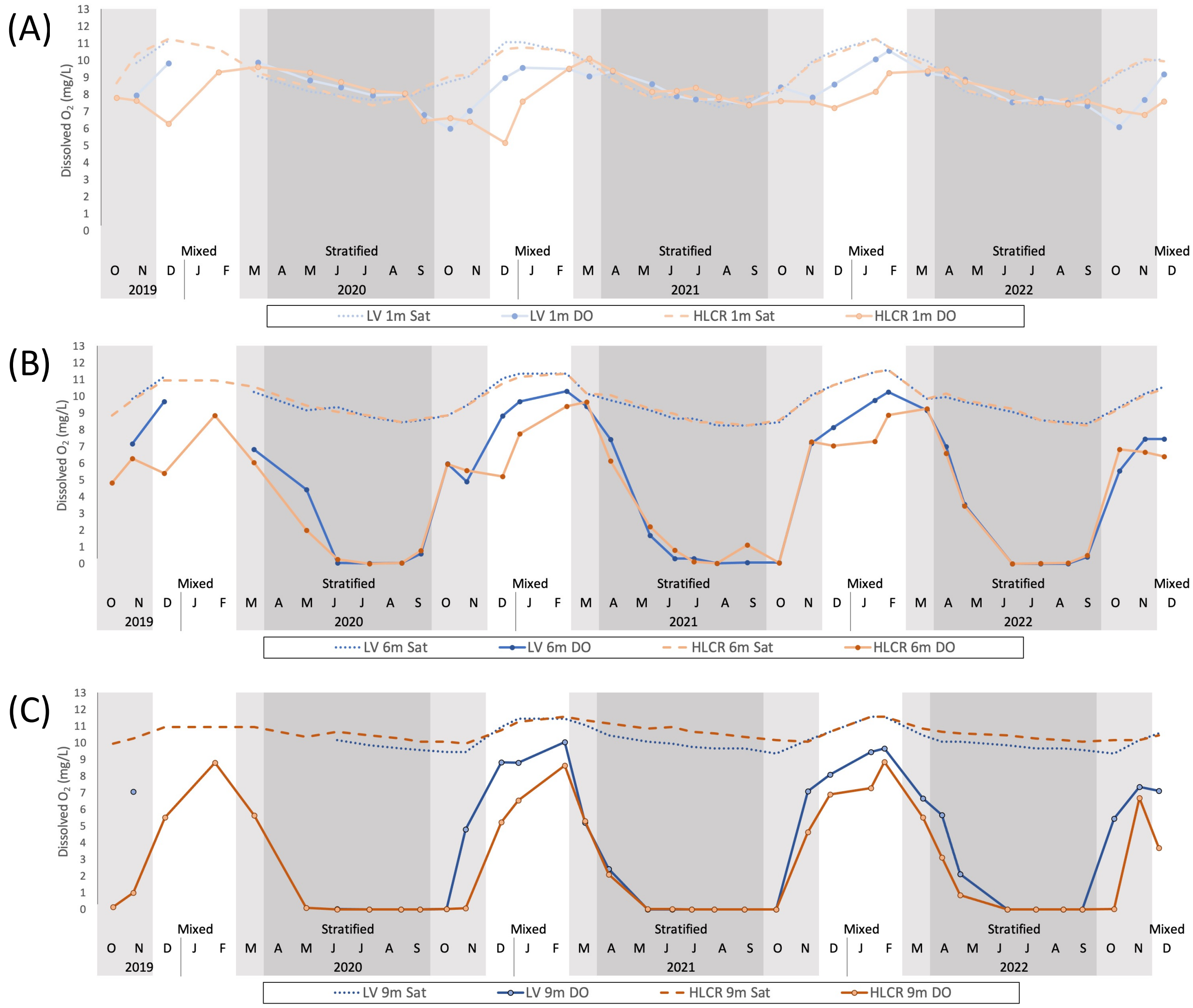

Figure 9. Dissolved oxygen (DO) concentrations in the epilimnion (A), metalimnion (B), and hypolimnion (C) for Lake Varner and Hard Labor Creek Reservoir compared with the oxygen saturation levels based on water temperature from October 2019 through February 2022. Fluctuation periods respond to the reservoirs' periods of mixing (white bars), transition (light grey bars), and stratification (dark grey bars). For ease of visualization, a particular depth was selected to represent each layer of the reservoir. While the exact depth of the thermocline, epilimnion, metalimnion, and hypolimnion changed throughout the period of thermal stratification, the thermal heatmap data indicate that it is overall appropriate to use a depth of 1 m to represent the epilimnion, a depth of 6 m to represent the metalimnion, and a depth of 9 m to represent the hypolimnion. Nearby depths show very similar patterns in each case.

(A) Lake Varner Nitrate

2020

Depth (m)	Jan	Feb	Mar	Apr	May	Jun	Jul	Aug	Sep	Oct	Nov	Dec
1	NA	0.5	0.2	0.3	0.3	0.4	0.5	0.2	0.2	0.9	0.2	1.4
3	NA	0.9	0.4	0.2	0.3	0.2	0.2	0.2	0.2	0.2	0.2	1.2
6	NA	0.6	B/D	0.3	0.4	0.1	0.1	0.1	0.1	0.3	0.1	0.5
9	NA	0.6	NA	NA	0.4	B/D	B/D	0.1	B/D	0.1	B/D	0.6

2021

Depth (m)	Jan	Feb	Mar	Apr	May	Jun	Jul	Aug	Sep	Oct	Nov	Dec
1	0.2	0.2	NA	NA	0.2	0.2	0.2	0.2	0.2	0.2	0.2	0.1
3	0.2	0.3	NA	NA	0.2	0.2	0.2	0.3	0.2	0.2	0.2	0.3
6	0.2	0.3	NA	NA	0.3	0.2	0.2	0.3	0.1	0.1	0.2	0.2
9	0.2	NA	NA	NA	0.2	0.1	0.2	0.1	B/D	0.4	0.1	0.2

2022

Depth (m)	Jan	Feb	Mar	Apr	May	Jun	Jul	Aug	Sep	Oct	Nov	Dec
1	0.4	0.1	0.4	0.2	0.1	0.3	0.3	0.2	B/D	0.2	0.2	B/D
3	0.2	0.2	0.3	0.1	0.2	0.3	0.1	0.2	0.2	0.2	0.2	0.2
6	0.1	0.2	0.4	0.2	0.3	0.3	0.3	0.3	0.3	0.2	0.2	0.2
9	0.1	0.1	0.2	0.1	0.2	0.4	0.2	B/D	B/D	0.3	0.2	0.2

(B) Hard Labor Creek Reservoir Nitrate

2020

Depth (m)	Jan	Feb	Mar	Apr	May	Jun	Jul	Aug	Sep	Oct	Nov	Dec
1	NA	0.8	0.7	2.6	0.5	0.3	0.2	0.2	0.2	5.1	0.3	3.9
3	NA	1.1	0.9	0.6	0.3	0.1	0.2	0.3	0.2	0.9	0.2	1.6
6	NA	0.6	0.4	0.5	0.4	0.3	B/D	B/D	0.2	0.4	0.2	1.5
9	NA	0.6	0.6	0.5	0.3	0.2	B/D	B/D	B/D	0.4	0.2	2

2021

Depth (m)	Jan	Feb	Mar	Apr	May	Jun	Jul	Aug	Sep	Oct	Nov	Dec
1	0.3	0.1	NA	NA	0.4	1.5	0.2	0.2	0.2	0.2	0.3	0.2
3	0.2	0.3	NA	NA	0.3	0.4	0.2	0.2	0.1	0.1	0.2	0.2
6	0.2	B/D	NA	NA	0.3	0.5	0.2	0.2	0.3	0.2	0.2	0.1
9	0.1	0.3	NA	NA	0.7	0.3	0.1	0.1	0.1	B/D	0.2	0.2

2022

Depth (m)	Jan	Feb	Mar	Apr	May	Jun	Jul	Aug	Sep	Oct	Nov	Dec
1	0.1	0.1	0.3	0.2	0.4	0.1	0.2	0.1	0.1	0.2	0.1	0.2
3	0.1	0.2	0.3	0.2	0.4	0.3	0.2	0.1	0.1	0.2	0.2	0.3
6	0.1	0.2	0.4	0.2	0.2	0.2	0.2	0.2	0.3	0.2	0.2	0.2
9	0.2	0.2	0.5	0.2	0.9	NA	0.1	0.1	0.1	0.2	0.1	0.2

(C) Lake Varner Total Phosphorus

2020

Depth (m)	Jan	Feb	Mar	Apr	May	Jun	Jul	Aug	Sep	Oct	Nov	Dec
1	NA	0.2	0.2	0.2	0.1	0.1	B/D	0.1	0.2	0.3	0.2	0.5
3	NA	0.2	0.2	0.2	0.1	0.2	B/D	0.1	0.2	0.2	0.2	0.6
6	NA	0.1	0.2	0.2	0.1	0.3	B/D	0.1	0.3	0.2	0.2	0.6
9	NA	0.2	NA	NA	0.2	0.1	B/D	B/D	0.1	0.1	0.1	0.5

2021

Depth (m)	Jan	Feb	Mar	Apr	May	Jun	Jul	Aug	Sep	Oct	Nov	Dec
1	1.0	0.3	NA	NA	0.1	0.1	0.1	0.7	0.1	0.1	0.8	0.7
3	1.0	0.4	NA	NA	0.1	B/D	0.1	0.7	0.4	0.1	0.1	0.2
6	1.1	0.4	NA	NA	B/D	0.1	0.2	0.6	0.5	0.1	0.1	0.2
9	1.0	NA	NA	NA	0.1	0.1	0.1	0.7	0.3	B/D	B/D	0.1

2022

Depth (m)	Jan	Feb	Mar	Apr	May	Jun	Jul	Aug	Sep	Oct	Nov	Dec
1	B/D	0.9	0.1	0.2	0.2	0.2	0.2	0.4	0.4	0.3	1.2	0.1
3	0.1	0.3	0.1	0.2	0.1	0.2	0.1	0.3	0.4	0.4	0.6	0.1
6	0.1	0.4	0.2	0.2	0.1	0.1	B/D	0.3	0.4	0.4	1.3	0.2
9	B/D	0.4	0.1	0.2	0.1	0.1	0.1	0.3	0.2	0.6	0.7	B/D

(D) Hard Labor Creek Reservoir Total Phosphorus

2020

Depth (m)	Jan	Feb	Mar	Apr	May	Jun	Jul	Aug	Sep	Oct	Nov	Dec
1	NA	0.2	0.1	0.2	0.1	0.2	B/D	0.2	0.3	0.3	0.3	0.4
3	NA	0.2	0.2	0.2	0.3	0.2	B/D	0.1	0.3	0.3	0.2	0.5
6	NA	0.1	0.1	0.2	0.1	0.1	B/D	0.2	0.3	0.2	0.2	0.5
9	NA	0.1	0.1	0.2	0.2	0.1	B/D	0.2	0.2	0.5	0.2	0.6

2021

Depth (m)	Jan	Feb	Mar	Apr	May	Jun	Jul	Aug	Sep	Oct	Nov	Dec
1	1.0	0.3	NA	NA	0.1	0.1	0.2	0.7	1.0	3.1	1.5	0.1
3	0.9	0.3	NA	NA	B/D	B/D	0.1	0.8	0.5	B/D	0.3	B/D
6	0.9	0.3	NA	NA	B/D	0.1	0.1	0.8	0.1	0.2	0.2	0.1
9	0.9	0.4	NA	NA	B/D	B/D	B/D	0.7	0.3	0.1	0.4	B/D

2022

Depth (m)	Jan	Feb	Mar	Apr	May	Jun	Jul	Aug	Sep	Oct	Nov	Dec
1	0.1	0.1	B/D	0.2	0.2	0.1	0.2	0.3	0.3	0.2	0.6	B/D
3	B/D	0.1	0.1	0.1	0.2	0.1	B/D	0.3	0.3	0.3	0.7	B/D
6	B/D	0.4	0.2	0.1	0.1	0.1	B/D	0.4	0.2	0.3	0.4	B/D
9	B/D	0.4	0.1	0.1	0.1	0.1	0.1	0.4	0.3	0.2	0.4	B/D

Scale mg/L
0.1
0.5
1
1.5
2
>2

Figure 10. Nitrate-nitrogen concentrations in Lake Varner (A) and Hard Labor Creek Reservoir (B), and phosphate concentrations in Lake Varner (C) and Hard Labor Creek Reservoir (D) collected monthly from 1, 3, 6, and 9 m depths. Times when data were not collected are represented by N/A. Times when the concentration was below the detection limit of the spectrophotometer are represented by B/D.

Hard Labor Creek Reservoir (HLCR)

Maximum NO_3^- –N concentrations were 5.1 mg/L (2020), 1.5 mg/L (2021), and 0.9 mg/L (2022) with 90% of values across all years being below 0.8 mg/L. During summer, concentrations were stable throughout the water column, however, in winter they generally decreased with depth. Generally, the lowest NO_3^- –N values were measured during the summer months. The highest NO_3^- –N concentrations throughout the water column were measured on December 17, 2020, when values ranged from 1.5 – 3.9 mg/L (Figure 10B).

Maximum PO_4^{-3}–P concentrations were 0.6 mg/L (2020), 3.1 mg/L (2021) and 0.7 mg/L, with 90% of values across all years being below 0.6 mg/L. Typically, no relationship was found between PO_4^{-3}–P concentration and depth, with values being relatively stable throughout the water column. Generally, the lowest PO_4^{-3}–P values were measured during the summer months. Higher concentrations were found throughout the water column in December 2020, January 2021, August 2021, and November 2022. The highest concentrations were found at 1 m depth in October and November 2021, at 3.1 mg/L and 1.5 mg/L, respectively (Figure 10D).

DISCUSSION

Temperature

Despite differences in lake size and depth and the presence or absence of solar-powered mixers, there is general consistency in the timing and depth of the onset of stratification between the two reservoirs. The onset of thermal stratification at the two reservoirs is within ± 2 days in 2020 and 2021 and within ± 9 days in 2022. While the depth of initial thermocline varies year to year, the thermocline occurs at the same depth in both reservoirs in all three years (Figures 3, 4, and 5). In LV, the thermocline temporarily disappeared from mid-April to mid-May 2020. The reason for the warming throughout the water column has yet to be determined.

While onset of thermal stratification occurred at the same time in both reservoirs, the timing of fall turnover differed slightly. In LV, where solar-powered mixers are present, the thermocline disappeared about one month earlier than in HLCR in all three years (Figures 3, 4, and 5). Because the timing of reservoir turnover is dependent on the size and depth of the lake (Wetzel 2001), the colder hypolimnetic waters found in the deeper HLCR relative to LV could be the driving cause for this difference. A study trying to create a model for predicting the date of fall turnover found that the best prediction could be achieved by using mean depth, adjusted latitude, and hypolimnetic temperature, with deeper lakes having colder hypolimnetic temperatures turning over later (Nürnberg 1988). However, we hypothesize that the presence of mixers in LV may also play a minor role. Solar-powered mixers are designed to only perform epilimnetic mixing. The intake for mixers in LV is located at 3 m depth, and when the thermocline is located below this depth it restricts vertical water mixing due to temperature-induced density differences. When temperatures cool in the fall, the epilimnion cools, the slope of the thermal gradient across the metalimnion decreases, and the thermocline gets deeper. Even though the depth of the solar mixer intakes remains constant, water from deeper in the water column can move upward towards those intakes as the thermal barrier is weakened. If the colder deep water is pumped to the reservoir's surface by the solar mixers, the turnover process may be accelerated, contributing to the faster autumn mixing observed in LV compared to HLCR.

Dissolved Oxygen (DO)

In both reservoirs, a clinograde oxygen profile is observed during thermal stratification, when the epilimnion (where photosynthesis dominates) is saturated and DO decreases with water column depth, approaching anoxia in the hypolimnion (where respiration dominates) (Figures 6, 7, and 8). During autumn mixing, DO monotonically increases at all depths. However, LV's DO levels increase at a faster rate than HLCR (Figure 9). The increase in DO was observed at all depths in all three years and is likely directly related to the more rapid thermal overturn, which can be attributed to the smaller size and shallower depth of LV relative to HLCR. We hypothesize that it might also be plausible that the solar-powered mixers may be a minor contributing factor in the oxygen dynamics. The earlier disappearance of the thermocline in LV allows the oxygen being produced in the epilimnion to begin mixing earlier, leading to the increase in concentration with depth. This increase in DO could also be the result of more photosynthesis occurring in LV, compared to HLCR.

Nutrients

Over the three-year study period, there were variable levels of both NO_3^- –N and PO_4^{-3}–P in both reservoirs, but no consistent patterns driven by seasonality or depth for either nutrient in either reservoir were found (Figure 10). For example, from spring to summer of 2020, NO_3^- –N levels generally decline across all depths in both reservoirs. However, in 2021 and 2022 the pattern does not hold, with low concentrations throughout the water column and throughout the year. While HLCR had several months in late 2021 with higher shallow-depth PO_4^{-3}–P concentrations than LV, levels are nearly identical between reservoirs for the same months and depths in 2020. Both reservoirs have a greater concentration of PO_4^{-3}–P throughout the water column in November 2022, but the same pattern is not found in 2020 or 2021. Without seasonal patterns, we began to investigate other potential sources of nutrient variation, either allochthonous or autochthonous.

Watershed area and land use are similar, with both being dominated by forest and grass/pastureland (Figure 2), suggesting that allochthonous nutrient input differences between the reservoirs should be minimal. DO can also influence nutrient dynamics. Both reservoirs experience periods of higher PO_4^{-3}–P concentrations, which has the potential to increase biological growth, as freshwater microbial populations are often phosphate limited. However, PO_4^{-3}–P increases are not consistently related to DO concentrations. We would expect PO_4^{-3}–P concentrations to increase in the summer when DO levels are lowest, especially in the hypolimnion where conditions are close to anoxic. While not measured directly in this study, it is likely that sediment pore water is also anoxic during times of hypolimnetic anoxia (Beutel 2003). If sediments experience periods of anoxia, the redox potential can become reducing, resulting in favorable conditions for P release into the water column (Moore, Jr. and Reddy 1994; Welch and Cooke 2005). This process could explain the higher levels of PO_4^{-3}–P measured in Aug. 2021 in both reservoirs and in Aug. 2020 in HLCR, as DO levels in the hypolimnion are close to 0 mg/L. However, we would expect to only see higher PO_4^{-3}–P levels below the thermocline due to the lack of mixing during thermal stratification (Welch and Cooke 2005), which is not the case. Additionally, both reservoirs also have higher levels of PO_4^{-3}–P in winter of all three years, when DO levels are increasing at their fastest rate. Based on this comparison of nutrient and DO data, it does not seem that the variations in nutrient dynamics are related to DO differences.

If the mixers were driving variation in nutrient dynamics between the reservoirs, we would expect to observe some consistent difference in nitrate or phosphorous concentrations, at least at certain times of year when we have established that the thermal stratification patterns are different (i.e., LV mixing more quickly in fall turnover than HLCR). However, no systematic differences between reservoirs are apparent, with both LV and HLCR lacking seasonal and depth patterns in nutrient concentrations (Figure 10). If we had found an allochthonous or autochthonous source of variation, it could be possible for the mixers to be counteracting that in some way, but no such source was identified. It is possible that a longer study may reveal more consistent patterns in nutrient dynamics, but with the data currently available, the similarities between nutrient concentrations throughout the year and water column between the reservoirs suggests that the mixers are not influencing nutrient dynamics.

Conclusions and Future Directions

While the impacts of solar-powered mixers on lake cyanobacterial populations in the epilimnion have been well studied, it is important to have a complete understanding of the potential impacts of the mixers on the physical and chemical dynamics of the entire lake water column as these mixers become more prevalent to mitigate or prevent HABs in lakes and drinking water reservoirs. While preliminary, the findings of this study suggest the impact of epilimnetic mixers on full lake thermal, oxygen, and nutrient processes in LV are minimal.

LV has been established for longer than HLCR, so we hypothesize that it might contain a more mature lacustrine biome. One study examining lakes and reservoirs in southern Italy found that in the absence of watershed agriculture and urbanization, planktonic communities tend to become more complex and to increase their species richness over time (Alfonso et al. 2010). Additionally, the mixers may be creating an environment where the phytoplankton community shifts from cyanobacterial to green algal and diatom dominant (Visser et al. 2016; Huisman et al. 2018; Reinl et al. 2021), and diatoms are among the most productive and environmentally flexible eukaryotic microalgae, typically having a greater productivity than other algal classes (Hildebrand et al. 2012). Water samples were collected and frozen during this study period, and future biological analysis of those samples may yield new findings about biodiversity, water chemistry, and nutrient dynamics.

Data collection is continuing, and additional years may clarify patterns or relationships, including how the reservoirs may be impacted by the long-term effects of climate change. Additional temperature arrays and collection locations in HLCR were established in September 2023 to better capture whole lake dynamics. This will be of particular importance for HLCR where it is likely that solar-powered mixers will be installed at some point in the next 1 – 5 years after a water treatment facility is constructed. We will then be able to have robust water column temperature, dissolved oxygen, and nutrient data before and after solar-powered mixer deployment to better compare the direct impacts.

ACKNOWLDEGEMENTS

We would like to thank Oxford College of Emory University for financially supporting this research. We would also like to thank the following student researchers that helped advance this project – Camilla Kline, Julia Danko, Yaling Covey, Ayaka Smart, and Stella Rae Kinard. Essential information about Lake Varner was provided by Bob Snipes, with the Newton County Water System, and about Hard Labor Creek Reservoir by Jimmy Parker, project manager for the reservoir. This manuscript was substantially improved thanks to the help of Dr. Sarah Cadieux, Emily Kelly, and several anonymous reviewers.

REFERENCES

About the Facility, Newton County, GA. 2022. https://www.co.newton.ga.us/223/About-the-Facility. (Accessed June 20, 2022).

Adrian, R., C. M. O'Reilly, H. Zagarese, S. B. Baines, D. O. Hessen, W. Keller, D. M. Livingstone, R. Sommaruga, D. Straile, E. Van Donk, G. A. Weyhenmeyer, and M. Winder. 2009. Lakes as sentinels of climate change. Limnology and Oceanography 54(6, part 2): 2283–2297. doi: 10.4319/lo.2009.54.6_part_2.2283.

Alfonso, G., G. Belmonte, F. Marrone, and L. Naselli-Flores. 2010. Does lake age affect zooplankton diversity in Mediterranean lakes and reservoirs? A case study from Southern Italy. Hydrobiologia 653: 149–164. doi: 10.1007/s10750-010-0350-4.

Atlanta Regional Commission. 2022. About the Atlanta Region. Atlanta Regional Commission.

Beutel, M. W. 2003. Hypolimnetic anoxia and sediment oxygen demand in california drinking water reservoirs. Lake and Reservoir Management 19(3): 208–221. doi: 10.1080/07438140309354086.

Boström, B., J. M. Andersen, S. Fleischer, and M. Jansson. 1988. Exchange of phosphorus across the sediment-water interface. Hydrobiologia 170(1): 229–244. doi: 10.1007/BF00024907.

Chislock, M., E. Doster, R. Zitomer, and A. Wilson. 2013. Eutrophication: causes, consequences, and controls in aquatic ecosystems. Nature Education Knowledge 4(4).

Conley, D. J., H. W. Paerl, R. W. Howarth, D. F. Boesch, S. P. Seitzinger, K. E. Havens, C. Lancelot, and G. E. Likens. 2009. Controlling Eutrophication: Nitrogen and Phosphorus. Science 323(5917). American Association for the Advancement of Science: 1014–1015. doi: 10.1126/science.1167755.

Cottingham, K. L., H. A. Ewing, M. L. Greer, C. C. Carey, and K. C. Weathers. 2015. Cyanobacteria as biological drivers of lake nitrogen and phosphorus cycling. Ecosphere 6(1): art1. doi: 10.1890/ES14-00174.1.

Cowie, G., M. Davis, S. Holmbeck-Pelham, M. Freeman, K. Freeman, K. Hatcher, R. Jackson, A. Miller Keyes, M. Merril, J. Meyer, E. Sutherland, and S. Wenger. 2002. *Reservoirs in georgia: meeting water supply needs while minimizing impacts*. UGA River Basin Science and Policy Center.

Elçi, Ş. 2008. Effects of thermal stratification and mixing on reservoir water quality. Limnology 9(2): 135–142. doi: 10.1007/s10201-008-0240-x.

Hach Company. 2014. Nitrate. Cadmium reduction method, Method 8171 (DOC316.53.01069). In Water Analysis Handbook, 9th ed. Loveland, CO: Hach Company.

Hard Labor Creek Regional Reservoir. Hard Labor Creek Regional Reservoir.

Hecky, R. E., and P. Kilham. 1988. Nutrient limitation of phytoplankton in freshwater and marine environments: A review of recent evidence on the effects of enrichment1. Limnology and Oceanography 33(4,part 2): 796–822. doi: 10.4319/lo.1988.33.4part2.0796.
Heisler, J., P. M. Glibert, J. M. Burkholder, D. M. Anderson, W. Cochlan, W. C. Dennison, Q. Dortch, C. J. Gobler, C. A. Heil, E. Humphries, A. Lewitus, R. Magnien, H. G. Marshall, K. Sellner, D. A. Stockwell, D. K. Stoecker, and M. Suddleson. 2008. Eutrophication and harmful algal blooms: A scientific consensus. Harmful Algae 8(1). HABs and Eutrophication: 3–13. doi: 10.1016/j.hal.2008.08.006.
Hildebrand, M., A. K. Davis, S. R. Smith, J. C. Traller, and R. Abbriano. 2012. The place of diatoms in the biofuels industry. Biofuels 3(2): 221–240. doi: 10.4155/bfs.11.157.
Ho, J. C., and A. M. Michalak. 2020. Exploring temperature and precipitation impacts on harmful algal blooms across continental U.S. lakes. Limnology and Oceanography 65(5): 992–1009. doi: 10.1002/lno.11365.
Hudnell, H. K. 2010. Within water-body management: a needed but neglected complement to watershed management. Clean Technologies and Environmental Policy 12(3): 205–207. doi: 10.1007/s10098-010-0304-6.
Huisman, J., G. A. Codd, H. W. Paerl, B. W. Ibelings, J. M. H. Verspagen, and P. M. Visser. 2018. Cyanobacterial blooms. Nature Reviews Microbiology 16(8). Nature Publishing Group: 471–483. doi: 10.1038/s41579-018-0040-1.
Hupfer, M., and J. Lewandowski. 2008. Oxygen controls the phosphorus release from lake sediments - a long-lasting paradigm in limnology. International Review of Hydrobiology 93(4–5): 415–432. doi: 10.1002/iroh.200711054.
Khan, F. A., and A. A. Ansari. 2005. Eutrophication: an ecological vision. The Botanical Review 71(4): 449–482. doi: 10.1663/0006-8101(2005)071[0449:EAEV]2.0.CO;2.
Maberly, S. C., J.-A. Pitt, P. S. Davies, and L. Carvalho. 2020. Nitrogen and phosphorus limitation and the management of small productive lakes. Inland Waters 10(2): 159–172. doi: 10.1080/20442041.2020.1714384.
Mesman, J. P., J. A. A. Stelzer, V. Dakos, S. Goyette, I. D. Jones, J. Kasparian, D. F. McGinnis, and B. W. Ibelings. 2021. The role of internal feedbacks in shifting deep lake mixing regimes under a warming climate. Freshwater Biology 66(6): 1021–1035. doi: 10.1111/fwb.13704.
Moore, Jr., P. A., and K. R. Reddy. 1994. Role of eh and ph on phosphorous geochemistry in sediments of Lake Okeechobee, Florida. Journal of Environmental Quality 23(5): 955–964.
Mortimer, C. H. 1941. The exchange of dissolved substances between mud and water in lakes. The Journal of Ecology 29(2): 280. doi: 10.2307/2256395.
Mortimer, C. H. 1942. The exchange of dissolved substances between mud and water in lakes. The Journal of Ecology 30(1): 147. doi: 10.2307/2256691.
Niedrist, G. H., R. Psenner, and R. Sommaruga. 2018. Climate warming increases vertical and seasonal water temperature differences and inter-annual variability in a mountain lake. Climatic Change 151(3): 473–490. doi: 10.1007/s10584-018-2328-6.
Nürnberg, G. K. 1988. A simple model for predicting the date of fall turnover in thermally stratified lakes. Limnology and Oceanography 33(5): 1190–1195. doi: 10.4319/lo.1988.33.5.1190.

O'Neil, J. M., T. W. Davis, M. A. Burford, and C. J. Gobler. 2012. The rise of harmful cyanobacteria blooms: The potential roles of eutrophication and climate change. Harmful Algae 14. Harmful Algae--The Requirement for Species-Specific Information: 313–334. doi: 10.1016/j.hal.2011.10.027.

O'Reilly, C. M., S. Sharma, D. K. Gray, S. E. Hampton, J. S. Read, R. J. Rowley, P. Schneider, J. D. Lenters, P. B. McIntyre, B. M. Kraemer, G. A. Weyhenmeyer, D. Straile, B. Dong, R. Adrian, M. G. Allan, O. Anneville, L. Arvola, J. Austin, J. L. Bailey, J. S. Baron, J. D. Brookes, E. de Eyto, M. T. Dokulil, D. P. Hamilton, K. Havens, A. L. Hetherington, S. N. Higgins, S. Hook, L. R. Izmest'eva, K. D. Joehnk, K. Kangur, P. Kasprzak, M. Kumagai, E. Kuusisto, G. Leshkevich, D. M. Livingstone, S. MacIntyre, L. May, J. M. Melack, D. C. Mueller-Navarra, M. Naumenko, P. Noges, T. Noges, R. P. North, P.-D. Plisnier, A. Rigosi, A. Rimmer, M. Rogora, L. G. Rudstam, J. A. Rusak, N. Salmaso, N. R. Samal, D. E. Schindler, S. G. Schladow, M. Schmid, S. R. Schmidt, E. Silow, M. E. Soylu, K. Teubner, P. Verburg, A. Voutilainen, A. Watkinson, C. E. Williamson, and G. Zhang. 2015. Rapid and highly variable warming of lake surface waters around the globe. Geophysical Research Letters 42(24): 10,773-10,781. doi: 10.1002/2015GL066235.

Paerl, H. W., N. S. Hall, and E. S. Calandrino. 2011. Controlling harmful cyanobacterial blooms in a world experiencing anthropogenic and climatic-induced change. Science of The Total Environment 409(10): 1739–1745. doi: 10.1016/j.scitotenv.2011.02.001.

Paerl, H. W., Karl. E. Havens, Nathan. S. Hall, T. G. Otten, M. Zhu, H. Xu, G. Zhu, and B. Qin. 2020. Mitigating a global expansion of toxic cyanobacterial blooms: confounding effects and challenges posed by climate change. Marine and Freshwater Research 71(5): 579. doi: 10.1071/MF18392.

Parker, A. 2019. Reservoirs. New Georgia Encyclopedia. September 3.

Reinl, K. L., J. D. Brookes, C. C. Carey, T. D. Harris, B. W. Ibelings, A. M. Morales-Williams, L. N. De Senerpont Domis, K. S. Atkins, P. D. F. Isles, J. P. Mesman, R. L. North, L. G. Rudstam, J. A. A. Stelzer, J. J. Venkiteswaran, K. Yokota, and Q. Zhan. 2021. Cyanobacterial blooms in oligotrophic lakes: Shifting the high-nutrient paradigm. Freshwater Biology 66(9): 1846–1859. doi: 10.1111/fwb.13791.

Reynolds, C. S. 2006. *The Ecology of Phytoplankton*. Cabridge University Press.

Rose, S., and N. E. Peters. 2001. Effects of urbanization on streamflow in the Atlanta area (Georgia, USA): a comparative hydrological approach. Hydrological Processes 15(8): 1441–1457. doi: 10.1002/hyp.218.

Schallenberg, M. D. Winton, P. Verburg, D. Kelly, K. Hamill, and D. Hamilton. 2013. Ecosystem services of lakes. In , 203–225.

Schindler, D. W., R. E. Hecky, D. L. Findlay, M. P. Stainton, B. R. Parker, M. J. Paterson, K. G. Beaty, M. Lyng, and S. E. M. Kasian. 2008. Eutrophication of lakes cannot be controlled by reducing nitrogen input: Results of a 37-year whole-ecosystem experiment. Proceedings of the National Academy of Sciences 105(32): 11254–11258. doi: 10.1073/pnas.0805108105.

Smucker, N. J., J. J. Beaulieu, C. T. Nietch, and J. L. Young. 2021. Increasingly severe cyanobacterial blooms and deep water hypoxia coincide with warming water temperatures in reservoirs. Global Change Biology 27(11): 2507–2519. doi: 10.1111/gcb.15618.

Stephenson, D. S. 2018. The tri-state compact: falling waters and fading opportunities. Florida State University Journal of Land Use and Environmental Law 16(1).

Sterner, R. W., B. Keeler, S. Polasky, R. Poudel, K. Rhude, and M. Rogers. 2020. Ecosystem services of Earth's largest freshwater lakes. Ecosystem Services 41: 101046. doi: 10.1016/j.ecoser.2019.101046.

Tammeorg, O., G. Nürnberg, J. Niemistö, M. Haldna, and J. Horppila. 2020. Internal phosphorus loading due to sediment anoxia in shallow areas: implications for lake aeration treatments. Aquatic Sciences 82(3): 54. doi: 10.1007/s00027-020-00724-0.

Upadhyay, S., K. A. Bierlein, J. C. Little, M. D. Burch, K. P. Elam, and J. D. Brookes. 2013. Mixing potential of a surface-mounted solar-powered water mixer (SWM) for controlling cyanobacterial blooms. Ecological Engineering 61: 245–250. doi: 10.1016/j.ecoleng.2013.09.032.

U.S. Geological Survey. 2013. USGS NED n34w084 1/3 arc-second 2013 1 x 1 degree IMG [raster digital data].

U.S. Geological Survey. 2019a. National Hydrography Dataset (ver. USGS National Hydrography Dataset Best Resolution (NHD) for Hydrologic Unit (HU) 03070101.

U.S. Geological Survey. 2019b. National Hydrography Dataset (ver. USGS National Hydrography Dataset Best Resolution (NHD) for Hydrologic Unit (HU) 03070103.

USDA National Agricultural Statists Service. 2019. CropScape, Cropland Data Layer [raster digital data].

USEPA. 1978. *Method 365.3: phosphorous, all forms (colorimetric, ascorbic acid, two reagent)*. Washinton, D.C.: United States Environmental Protection Agency.

Visser, P. M., B. W. Ibelings, M. Bormans, and J. Huisman. 2016. Artificial mixing to control cyanobacterial blooms: a review. Aquatic Ecology 50(3): 423–441. doi: 10.1007/s10452-015-9537-0.

Wagner, C., and R. Adrian. 2009. Cyanobacteria dominance: Quantifying the effects of climate change. Limnology and Oceanography 54(6, part 2): 2460–2468. doi: 10.4319/lo.2009.54.6_part_2.2460.

Welch, E. B., and G. D. Cooke. 2005. Internal phosphorus loading in shallow lakes: importance and control. Lake and Reservoir Management 21(2): 209–217. doi: 10.1080/07438140509354430.

Wetzel, R. G. 2001. *Limnology: Lake and reservoir ecosystems*. Academic Press.

Williamson, C. E., J. E. Saros, W. F. Vincent, and J. P. Smol. 2009. Lakes and reservoirs as sentinels, integrators, and regulators of climate change. Limnology and Oceanography 54(6part2): 2273–2282. doi: 10.4319/lo.2009.54.6_part_2.2273.

Yang, Y., Y. Wang, Z. Zhang, W. Wang, X. Ren, Y. Gao, S. Liu, and X. Lee. 2018. Diurnal and seasonal variations of thermal stratification and vertical mixing in a shallow fresh water lake. Journal of Meteorological Research 32(2): 219–232. doi: 10.1007/s13351-018-7099-5.

Zhong, S., Y. Geng, Y. Qian, W. Chen, and H. Pan. 2019. Analyzing ecosystem services of freshwater lakes and their driving forces: the case of Erhai Lake, China. Environmental Science and Pollution Research 26(10): 10219–10229. doi: 10.1007/s11356-019-04476-9.